Journal for Nature Conservation 62 (2021) 126020

Contents lists available at ScienceDirect

Journal for Nature Conservation

journal homepage: www.elsevier.com/locate/jnc

Using drone imagery analysis in rare plant demographic studies

Kody R. Rominger [a], Alyson DeNittis [a], Susan E. Meyer [b,*]

[a] Department of Biology, Utah Valley University, 800 West University Parkway, Orem, Utah, 84058, USA
[b] USDA Forest Service, Rocky Mountain Research Station, Shrub Sciences Laboratory, 735 North 500 East, Provo, Utah, 84606, USA

ARTICLE INFO

Keywords:
Arctomecon humiliss
Dwarf bear poppy
Population monitoring
Rare plant conservation
Unmanned aerial vehicle (UAV)

ABSTRACT

For plant species of conservation concern, knowledge of changes in abundance through time is a minimum requirement for informed management. This information is usually acquired through on-the-ground monitoring, which entails counting individuals in defined areas over multiple years. Demographic studies, which involve tracking individual plants through time, are usually carried out at limited spatial scales and over shorter time frames than monitoring, but are more useful to management. In this study we explored the use of drone (UAV or unmanned aerial vehicle) imagery analysis as a tool for collecting demographic data for dwarf bear poppy (*Arctomecon humilis*), an endangered species restricted to gypsum outcrops in the northeastern Mojave Desert, USA. We obtained imagery at 15 m altitude during peak flowering at four populations in spring 2019. Each poppy plant in the imagery was georeferenced, measured and scored for flowering. To estimate reproductive output, we developed independent data sets relating plant diameter to flower number, then sampled to determine mean fruit set per flower and seeds per fruit. We used these relationships along with plant diameter and reproductive status for each plant in the drone imagery to estimate seed rain on an area basis across nine 0.6 ha demography plots at each population. This method enabled us to collect demographic data on >3,000 plants, including estimated production of ca. 3.7 million seeds, across >20 ha of habitat. We also analyzed imagery acquired in both 2018 and 2019 at two of the four populations and quantified recruitment, growth, and mortality of individual georeferenced plants. Our study is among the first to demonstrate the utility of drone imagery analysis in plant demographic studies. The method is most applicable for non-clonal perennial species with distinctive morphology that occur in habitats with low vegetative cover.

1. Introduction

Population monitoring is perhaps the most fundamental activity involved in the management of plants of conservation concern. It is one of a series of evaluation methods that usually take place at successively finer spatial scales. The terminology applied to these methods varies (Elzinga, Salzer, Willoughby, & Gibbs, 2009; Menges & Gordon, 1996; Palmer, 1987), but in general the following definitions apply. Survey is evaluation at the broadest scale and is aimed primarily at documenting species occurrence at the population level, including the discovery of new populations or verification of population presence in a specific management context. Census is aimed at enumerating individuals within a population. It can include classification by life stage (e.g., juvenile, nonflowering adult, flowering adult). Monitoring is aimed at detecting population trends through time. This usually involves counting individuals, again sometimes by life stage, in smaller defined areas within a population at multiple points in time, often with yearly evaluation. Finally, demographic studies are aimed at measuring demographic variables, e. g., recruitment, survival, and reproductive status, that are useful in population modeling. These studies involve repeated evaluation of individual plants rather than enumeration of individuals in a defined area each year. Demographic studies are more labor-intensive than monitoring and are usually carried out at smaller spatial scales.

Evaluations for determining the status of rare plant species are typically conducted on the ground by managers, contractors, or researchers. Because of limited funding available for plant conservation, demographic studies in particular are often limited in scope or not performed at all, even though demographic data are potentially highly useful for management. The recent advent of powerful but reasonably priced drone (UAV, unmanned aerial vehicle) technology has introduced the possibility of demographic data collection from drone imagery rather than on the ground (Baena, Moat, Whaley, & Boyd, 2017; Baena, Boyd, & Moat, 2018; Sanchez-Bou & Lopez-Pujol, 2014). If feasible, this

* Corresponding author.
E-mail address: Susan.Meyer@usda.gov (S.E. Meyer).

https://doi.org/10.1016/j.jnc.2021.126020
Received 26 December 2020; Received in revised form 5 May 2021; Accepted 12 May 2021
Available online 21 May 2021

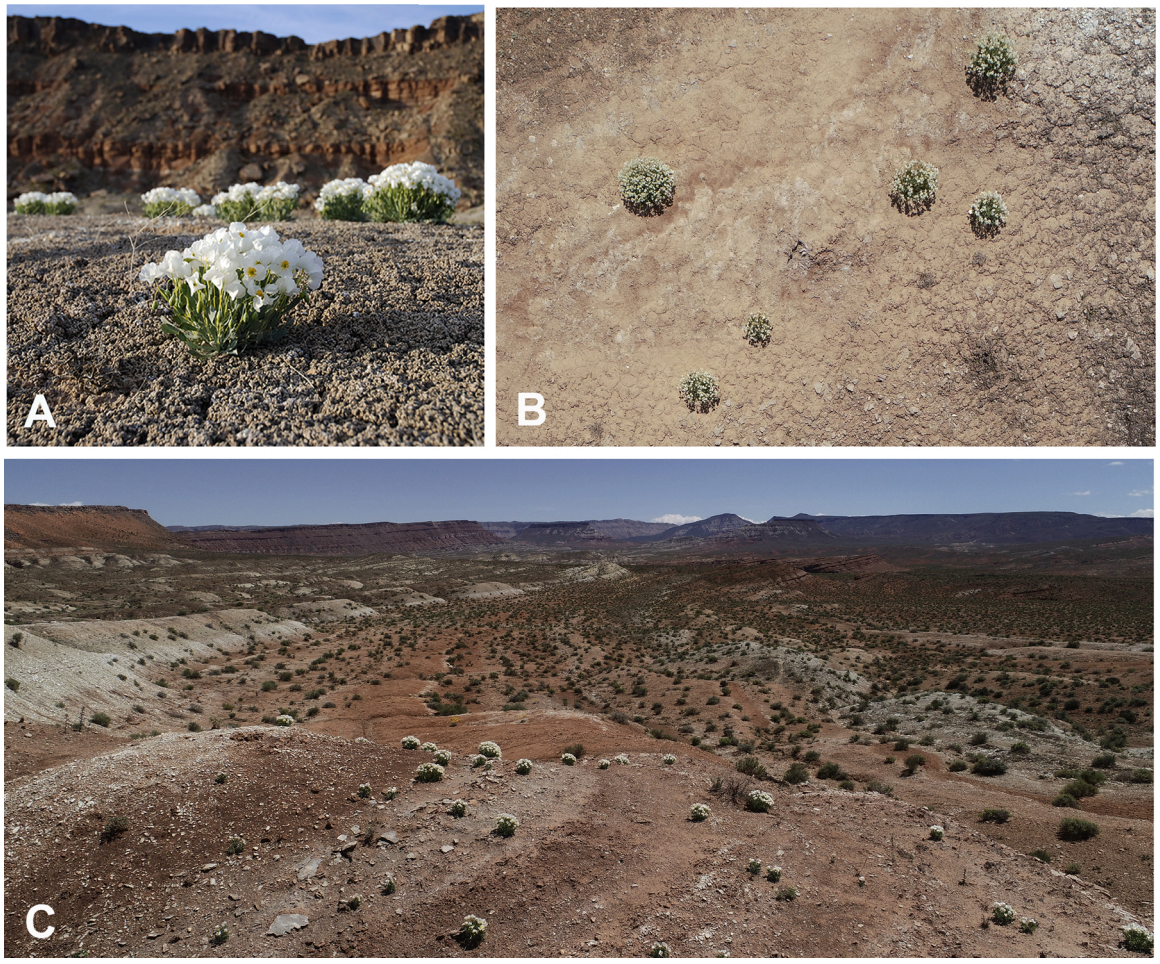

Fig. 1. A. Dwarf bear poppies in flower at the Red Bluffs (Tonaquint) population in May 2009 (photo: Renee Van Buren), B. Dwarf bear poppies in flower as they appear in the imagery obtained at 15 m altitude, C. Dwarf bear poppy demography plot at the Beehive Dome population in May 2019 (photo: Kody Rominger).

could have numerous advantages, including reduced field time, labor, and cost, the ability to monitor in inaccessible habitats, less surface disturbance especially in fragile habitats, and the potential to sample much larger areas and to quantify demographic parameters for larger numbers of individuals. Drones are now extensively used in conservation biology, with considerable emphasis on wildlife (Christie, Gilbert, Brown, Hatfield, & Hanson, 2016; Fust & Loos, 2020). For plants, much of the work has involved mapping cover of invasive species (Dash, Watt, Paul, Morgenroth, & Hartley, 2019) or vegetation mapping more generally (e.g., Cunliffe, Brazier, & Anderson, 2016; Zweig, Burgess, Percival, & Kitchens, 2015). In a recent review, Cerrejón, Valeria, Marchand, Caners, and Fenton (2021)) discussed the current state of research on use of drone imagery for rare plant detection. A few published papers have used drone imagery for plant census (e.g., Leduc & Knudby, 2018; Ouyang et al., 2020; Strumia, Buonanno, Aronne, Santo, & Santangelo, 2020; Van Auken & Taylor, 2017), but reports of its use for studies at a finer scale in natural systems are scarce. The few examples we found involved tracking seedling or sapling fate over short time scales in semi-natural settings (Buters, Belton, & Cross, 2019; Feduck, McDermid, & Castilla, 2018).

Edaphic endemics make up a sizeable fraction of plant species of conservation concern, occurring worldwide on limestone-derived soils (Willis, Cowling, & Lombard, 1996), serpentine-derived soils (Anacker, 2014), and gypsiferous soils (Escudero, Palacio, Maestre, & Luzuriaga, 2015; Pérez-García et al., 2017), among others. These edaphic environments usually support relatively simple plant communities with low vegetative cover even in more mesic habitats, increasing the likelihood that drone technology could successfully be employed. This indicates that a methodology for carrying out demographic studies using drone imagery could have wide application in plant conservation.

We previously utilized drone technology for census of a globally endangered species, dwarf bear poppy (*Arctomecon humilis* Coville), an edaphic endemic restricted to gypsum outcrops at the northeastern edge of the Mojave Desert, USA (Rominger & Meyer, 2019). This species is conspicuous in flower, has a distinctive morphology, and occurs in habitats with sparse vegetative cover, making it a promising candidate for further drone imagery analysis (Fig. 1). In the work reported here, we examined the feasibility of carrying out drone-based demographic studies for dwarf bear poppy. Our principal short-term objective was to test the following hypotheses regarding the utility of drone imagery analysis for fine-scale status evaluation for this species:

1) Drone imagery can be used to locate, identify, count, measure and determine reproductive status of individual poppy plants ≥6 cm in diameter in demography plots, and these data can be used to characterize plant density, size class distribution, and population-level reproductive status.
2) Small-scale on-the-ground studies to determine diameter, flower number, fruit set and seeds per fruit on a sample of individual plants at each population will make it possible to estimate seed number per flower and per plant.
3) The relationship between plant diameter and flower number obtained in small-scale studies will enable estimation of flower number for plants measured in drone imagery.

Table 1
Demography study location and site data (See United States Fish & Wildlife Service, 2016 for map of population locations).

	Demography Site			
	Beehive Dome	Shinob Kibe Preserve	Tonaquint Block	White Dome Preserve
Main Population	Beehive Dome	Shinob Kibe	Red Bluffs	White Dome
Land Ownership	BLM[a]	TNC [b], BLM, private	BLM, SITLA[c], tribal	TNC, SITLA
Monitoring Area	75 ha	4.13 ha (poppy habitat, TNC Preserve)	166 ha	325 ha (TNC Preserve)
Management	Closed to motorized travel, non-motorized allowed; seasonal cattle use	Officially closed except for research but with frequent foot and mountain bike trespass	Closed to motorized travel, non-motorized allowed; some seasonal cattle use; heavily disturbed in some areas, high use by mountain bikes	Closed to motorized travel since preserve was established in 2007; only hiking on designated trails allowed; no public access to designated research areas.

[a] US Department of the Interior, Bureau of Land Management.
[b] The Nature Conservancy.
[c] Utah State School Trust Lands.

4) Flower number combined with quantification of mean seeds per flower can be used to estimate seed production per plant for each flowering plant in the drone imagery.
5) Estimates of seed production per plant can then be combined with density and size class distribution data to calculate seed production in demography study plots on an area basis, i.e., seed rain.
6) Comparing individual georeferenced poppy plants in drone imagery obtained in two consecutive years will enable quantification of additional demographic parameters, including recruitment, survival, growth or size regression, and change in reproductive status.
7) Drone-based demographic studies will demonstrate among-population differences and trends through time within populations, increasing our knowledge of species biology and alerting managers to potential problems at the population level.

2. Methods

2.1. Species description

Dwarf bear poppy was listed as federally endangered in 1979 (United States Fish & Wildlife Service, 1979). All species occurrences are restricted to gypsiferous soils and lie within a 15 km radius of St. George, Utah, USA, a rapidly growing urban area at the northeastern edge of the Mojave Desert. A perennial plant that can live up to ten years, dwarf bear poppy reproduces exclusively from seed. In the 16-year demographic study of Harper and Van Buren (2004), seedling emergence occurred episodically in response to >50 mm of late winter-spring precipitation. First-year seedlings were tiny (2 cm mean diameter) and did not flower, while yearling plants averaged 5 cm in diameter and approximately a quarter of these yearlings flowered. Adult plants average 20 cm in diameter but can grow as large as 60 cm. They have strong taproots topped by a branched caudex with clumps of basal leaf rosettes (Fig. 1). The plants keep their leaves year-round, growing by adding new rosettes each spring. Larger plants may remain static or regress in size as older clumps of rosettes senesce and die. Flowers are produced from branched reproductive stalks that emerge from the leaf axils in late spring, and most plants of reproductive size flower profusely even in years with suboptimal spring precipitation. Seeds are produced in apically dehiscent capsules that can be dispersed by wind inside the papery dried flowers, which break from the pedicel at capsule maturity. Seed production is variable but is often high, and some seeds are produced almost every year (Harper & Van Buren, 2004; Harper, Van Buren, & Aanderud, 2001; Portman, Tepedino, Tripodi, Szalanski, & Durham, 2018; Tepedino, Mull, Griswold, & Bryant, 2014). These form a persistent seed bank that provides for episodic recruitment in response to favorable establishment conditions in subsequent years (Meyer, Van Buren, & Searle, 2015).

2.2. Demography plot design and selection

2.2.1. One-year study – 2019

Locations were selected for the first year of long-term demography studies from within four recently drone-censused populations (Rominger, 2018, 2019a, 2019b; Rominger & Meyer, 2019; Table 1). We used a stratified random sampling method to determine the placement of the demography plots within each population. To avoid bias that might result from sampling only high-density areas, we took advantage of plant distribution data from the 2018 census to stratify the area occupied by each population into high, medium, and low relative density classes. Using ArcMap 10.7 (ESRI, Redlands, CA), we calculated kernel density independently for each population using previously acquired poppy presence data. Density was then broken into four classes (high, medium, low, negligible) using the natural breaks method. The "negligible" class was used only to mask very low-density and unoccupied areas. This resulted in three ranked density classes that had unique sets of density values for each population.

At the Beehive Dome and Tonaquint populations, we randomly selected three locations within each density class for a total of nine demography plots. Each plot was 40 × 150 m (0.6 ha) and was positioned to include the maximum number of plants within the respective density class area. At the White Dome population, we randomly selected three previously established 0.1 ha Abella monitoring plots (Abella, 2012,) within each density class. We positioned each of the nine 40 × 150 m demography plots so that it completely encompassed the respective 20 × 50 m (0.1 ha) Abella plot (for reasons explained below) and included as much of the density class as possible. At the Shinob Kibe Preserve, which is only 4.13 ha in total area, we divided the area into nine demography plots of approximately equal size (ca. 0.47 ha). These plots were ranked using counts from the 2018 census (Rominger, 2018) to obtain three density classes and evaluated along with demography plots at the other three populations in 2019. We also used 2019 imagery from previously established 0.1-ha plots within the full-size plots at White Dome and Shinob Kibe to enable density comparisons between plot sizes in 2019.

2.2.2. Two-year study – 2018/2019

We used the Abella plots at White Dome as a basis for our demographic comparison across years because previously analyzed 15 m imagery was available for these smaller plots from an independent study carried out in 2018 (Rominger, 2018). We also made use of previously analyzed 15 m imagery from 2018 available for the entire Shinob Kibe Preserve (Rominger, 2018). This made it possible to examine recruitment, survival, and growth of individual poppies across two years at two populations. We could then evaluate the potential value of drone-based year-to-year demographic data in addition to the data generated in a one-year study.

2.3. Mission planning and flights

All drone flights were conducted using the DJI Phantom 4 Pro V2 (SZ DJI Technology Co. Ltd. Shenzhen, China) with stock camera (f/2.8-f/11, 84°_ FOV, 20 M P). The drone controller was interfaced with a Samsung Galaxy Tab A (Samsung, Seoul, South Korea). Individual flights

were planned and carried out using the Drone Harmony android app (Drone Harmony, Luzern, Switzerland). This specific application was chosen because it allows for the import of elevation data which is used to maintain consistent drone altitude above ground level. We used 5-m autocorrelated DEM as the elevation data source (Utah Automated Geographic Reference Center), which was the highest resolution elevation data available for our study area.

All drone flights were conducted at 15 m altitude. Demography plots were flown individually at Beehive Dome, Tonaquint, and White Dome, while the Shinob Kibe Preserve was flown in its entirety. We carried out a total of 40 flights in April-May 2019, during peak poppy flowering. These flights resulted in over 5,500 images captured across all populations.

2.4. Image processing

UAV-captured images were sorted by population, purpose, year, and flight number, and stored in an external hard drive. All images were standardized to minimize color and light distortion. We used the Photoshop (Photoshop CC 2019, Adobe Systems Inc., San Jose, CA, USA) tools "neutralize" and "match color" to adjust pixel values for color and light for all images within an individual flight. The colors were matched relative to a template image from the target flight that was manually adjusted with the camera raw filter to maximize poppy visibility. Each flight had a template image adjusted to the unique field conditions of that particular flight.

After color standardization, images from each flight were further processed using Pix4D software (Pix4D S.A., Lausanne, Switzerland) to generate high-resolution orthomosaics. The orthomosaic outputs were then imported into ArcMap (ESRI, Redlands, CA) for analysis. The average ground sampling distance (GSD) of the demography plot flights was similar across locations: 0.503 ± 0.044 cm/pixel at Beehive Dome, 0.577 ± 0.015 cm/pixel at Shinob Kibe, 0.482 ± 0.039 cm/pixel at Tonaquint, and 0.519 ± 0.028 cm/pixel at White Dome. The differences in GSD were due mainly to differences in flight planning elevation data resolution.

2.5. Demography plot image evaluation

In ArcMap, fishnet grids were generated across each demography plot in the 2019 imagery (2.5 m row height). The plot orthomosaic was then visually scanned back and forth across each grid row at a scale of 1:15. When a poppy was encountered it was digitally marked, measured at maximum diameter and classified by reproductive status (non-flowering or flowering). A similar procedure was followed for the 2018 imagery from White Dome (Abella plots) and Shinob Kibe (full-size plots).This method may generate some error due to resolution differences and limitations, but this error is expected to be small. We determined that the threshold diameter for reliable identification of poppies across all the imagery was 6 cm. Thus poppies <6 cm in diameter were excluded from current-year populations even when visible in the imagery. These plants were considered not yet recruited into the population, regardless of their age. This was justifiable because plants <6 cm almost never flower or contribute seeds to future generations (Harper & Van Buren, 2004), so that their presence has essentially no immediate demographic impact.

2.6. Reproductive output field sampling

Plants for reproductive output studies included all the flowering individuals from one high-density plot each at White Dome, Beehive Dome, and Tonaquint, for a total of ca. 100 plants per population. At Shinob Kibe, plants were selected from across the Nature Conservancy Preserve (Table 1). Each of ca. 100 plants at each population was identified with a numbered metal tag stapled into the adjacent ground and its approximate GPS location was recorded. Sampling occurred during peak flowering time, at the same time as drone imagery capture. Maximum diameter for each plant was measured and open flowers and buds were counted to obtain maximum flower number.

We had planned to use the tagged plants to ground-truth poppy identifications and size measurements in the drone imagery as needed, but our ground GPS coordinates were not sufficiently accurate to permit reliable matching with plants in the imagery. We later solved this problem *ex post facto* in the field by matching accurately located plants in the 2019 drone imagery with plant tags from 2019 in the field using the tablet application Avenza (Avenza Systems Inc., Toronto, Canada), which created a track on the drone imagery as we walked from plant tag to plant tag. This made it possible to accurately match individual plants in the imagery with measurements from field-tagged plants.

After fruit (capsule) formation was complete but before dehiscence, capsules on each plant were counted to determine fruit set (number of fruits/number of flowers). Five percent of the capsules were then collected for seed quantification. This fraction was harvested from each plant according to its size so that smaller plants were not stripped of most or all of their capsules. This fraction was chosen to obtain a sufficient sample size for accurate estimation of seed production but also to minimize seed removal from the site. Filled seeds, aborted seeds, and unfertilized ovules were enumerated for each capsule. Viability of 100 filled seeds from a bulk collection at each population was obtained by tetrazolium staining (Ooi, Auld, & Whelan, 2004) and averaged 96 % (S. Clement, unpublished data). Filled seed data were used in subsequent analyses because of the uniformly high viability and the lack of viability information on a per plant basis.

2.7. Analysis and interpretation

We used SAS 9.4 (SAS Institute, Cary NC) Proc Glimmix for analysis of variance (ANOVA) of data sets with binomial response variables and SAS 9.4 Proc GLM for data sets with continuous response variables, except as otherwise stated. The latter were transformed as needed to meet normality and homogeneity of variance assumptions. *A posteriori* means separation tests represent pre-planned least significant difference tests in LSMeans from each analysis. Details of analysis are presented in Appendix A in tables that are referenced in the methods and results section for each data set and also in their respective data tables. The polynomial regression analysis on plant maximum diameter versus flower number was performed in JMP (SAS Institute, Cary NC) (see full methods below).

2.7.1. Demography plot imagery interpretation

Data from the 2019 drone imagery were summarized for each plot to determine poppy density, size class distribution, and reproductive status. We used analysis of variance (ANOVA) based on poppy count data from the nine plots at each population to determine if density varied as a function of population or *a priori* density class (See Appendix A Table A1). We also performed ANOVA to determine whether plant density was related to plot size for Shinob Kibe and White Dome, the two populations where data from two plot sizes were available (See Appendix A Table A2). We used plant diameter measurements to construct size class distributions based on 5 cm diameter increments for pooled data from full-size plots for each population and also to calculate mean, mode, and median plant diameters for each population. We then calculated the proportion of plants that were flowering for each population overall and also by size class. We also tested for significant differences among populations in mean diameter (Table A3)

2.7.2. Reproductive output study interpretation

We examined the relationship between flowering plant diameter and total flower number (including buds) in the field data for each population using nonlinear regression. Exploratory curve-fitting for a suite of polynomial equations using the Fit Curve Platform in JMP resulted in selection of second-order polynomial regression equations that provided

the best fit to the flowering data across the range of values encountered in each population. This made it possible to estimate flower number for individual plants based on diameter measurements from the drone imagery.

We also performed regression analysis on a set of plants at Beehive Dome with matched field-based and imagery-based diameter measurements from 2019 to evaluate the degree to which these two methods produced comparable results (Appendix B). Perfect congruence would result in a regression line of slope 1 and intercept 0 and a coefficient of determination (R^2) of 1.

Fruit set values for each plant (fruit number/flower number) were used in ANOVA to determine whether there were differences among populations in mean fruit set (Table A4a). To examine differences in number of seeds per fruit, we first calculated mean number of seeds per fruit for each plant. Because more capsules were collected from larger plants, using capsule as an experimental unit could have skewed the results. We then used ANOVA to determine whether there were differences in mean seed number per capsule among populations (Table A4b). Finally, we estimated mean seed number per flower at each population by multiplying mean fruit set (fruits/flower) by mean seeds/fruit.

We used the polynomial equations described previously for each population to estimate flower number for every flowering plant in the 2019 imagery-derived demography data set based on its maximum diameter. Estimated flower number for each plant in a population, including zeroes for nonflowering plants, was then multiplied by mean seeds per flower for that population to obtain an estimate of seed production for each plant. Total seed production on each demography plot was then obtained by summing seed production per plant for each plot.

We also calculated mean seed production per flowering plant at each population and estimated seed production by size class by summing seed production for all plants within each size class and calculating mean, modal, and median plant size for seed production. Mean seed production plant size was interpreted as the plant size that corresponded to mean seed production, whereas median seed production plant size was the diameter of the plant with seed production at the midpoint of plants ranked by seed production. Modal plant size for seed production was interpreted as the midpoint of the class with the highest seed production.

Lastly, we calculated seed rain per unit area within the plots at each population by dividing total seed production by total area. We used ANOVA to analyze differences in seed production per plot as a function of population and density class (Table A5a) and differences among populations in seed production per plant (Table A5b).

2.7.3. Demographic analysis across years

To examine demographic changes across years at White Dome and Shinob Kibe, we compared each marked and georeferenced plant across the 2018 and 2019 imagery. It was straightforward to compare individuals between years to determine whether they survived from 2018–2019. An individual marked as present in 2018 but not in 2019 was presumed dead. A poppy present in 2019 that was not marked in the 2018 imagery was presumed present in 2018. A close reexamination of the 2018 imagery frequently revealed some indication that the plant was indeed present, but was not big enough to be reliably identified and therefore was not marked (i.e., diameter <6 cm). These plants were considered to be new recruits in 2019, i.e., recruited into the size class range that could be accurately evaluated, but they were excluded from the 2018 data set used to calculate survival. This was necessary to avoid systematic error in the survival estimate, as there was no way to determine the number of plants too small to identify and mark in 2018 that did not survive to 2019. There was likely no seedling survival or even emergence in the very dry spring of 2018, so any plants present in 2018 were at least yearlings and potentially visible in the imagery that year. Plants newly detected in 2019 could not be current-year seedlings, because these are well below the threshold of detectability (Harper & Van Buren, 2004).

We calculated overall survival of recruited plants (≥6 cm) across years at each of the two sites and obtained size class distributions for each year from plant diameter as described earlier. We also examined survival as a function of 2018 size class, and determined how individual plant sizes changed across years, both as growth interval (change in diameter) and proportional growth (2019 diameter/2018 diameter). We examined proportional growth as a function of 2018 diameter for each population and also calculated the proportion of individuals that regressed in size. Plants that recruited in 2019 were included in the growth calculations by assuming a 2018 diameter of 5 cm, the mean diameter of yearling plants in Harper and Van Buren (2004).

Table 2
Total plant number and density on nine full-size demography plots[1], three in each of three *a priori* density classes, at each of four populations of *Arctomecon humilis* in 2019. Population and density class main effects were highly significant ($P = 0.0004$ and $P < 0.0001$, respectively, in two-way ANOVA, while the interaction between population and density class was not significant. (See Table A1 for full analysis).

Population	Total plant number	Overall density (plants-ha^{-1})	*A priori* density class mean density (plants-ha^{-1})		
			Low	Med	High
Beehive Dome	750	138.9 ± 23.9a	73.3	133.3	210.0
Shinob Kibe	270	64.2 ± 19.2b	14.6	32.9	132.3
Tonaquint	1095	202.8 ± 43.4a	73.9	217.8	316.7
White Dome	924	171.1 ± 63.3a	38.3	105.6	369.4
Mean ± SE	759.8 ± 152.6	144.2 ± 21.6	49.8 ± 10.8c	125.5 ± 23.2b	257.7 ± 42.2a

[1] Full-size plots were 0.6 ha in size except at Shinob Kibe where they varied slightly in size and averaged 0.47 ha (see text for explanation). Means separations significant at $P < 0.05$. Error bars represent standard error of the mean.

Table 3
Mean plant densities (± standard errors) expressed as plants per hectare on demography plots of two sizes. Based on ANOVA the plot size main effect was significant at $P = 0.0009$, while the site main effect and site by plot size interaction were not significant (See Table A2 for full analysis).

Site	Abella plots (0.1 ha) Plants-ha^{-1}	Full-size plots[1] Plants-ha^{-1}
Shinob Kibe	237.8 ± 63.8	64.2 ± 19.2[1]
White Dome	486.7 ± 198.8	171.1 ± 63.3
Mean	362.2 ± 105.7a	117.7 ± 34.6b

[1] Full-size plot size at Shinob Kibe was variable and averaged 0.47 ha; at White Dome full-size plots were 0.6 ha.

3. Results

3.1. One-year study (2019)

3.1.1. Sample size, plot size, and plant density

The average total sample size across nine full-size demography plots at the four study populations was 760 plants for a total of 3039 plants across all populations (Table 2; see ES1 for full data set). Because plots were similar in area, sample size varied by population as a function of plant density within the plots (see Table A1 for analysis). Mean density was significantly lower at Shinob Kibe than at the other three populations (Table 2).

There were also significant differences across all populations in mean plant density among three *a priori* density classes established on the basis of previously obtained census data. These differences were in the rank order high > medium > low density as predicted (Table 2, Table A1). The relative differences among high, medium, and low density classes were similar across sites (no significant population by density class interaction). This analysis validated our approach to selection of plots in areas of contrasting plant density.

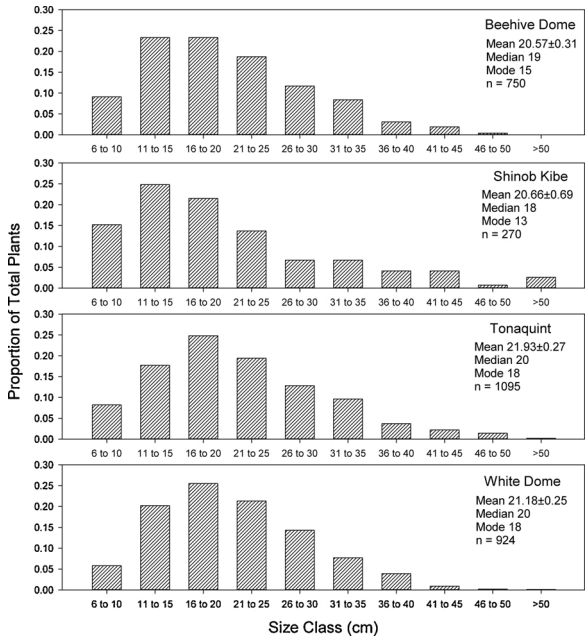

Fig. 2. Size class distributions pooled across full-size demography plots at four populations of *Arctomecon humilis* evaluated in 2019. Mean diameter ± standard error, median diameter, and modal diameter are presented on the graph for each population.

In comparisons between the two plot sizes at two sites, plant number increased with plot size but was not proportional to the increase in plot size because there was a highly significant effect of plot size on density, with much higher densities in Abella (0.1 ha) plots compared with full-size plots at both White Dome and Shinob Kibe (Table 3, Table A2). Poppies are highly clustered in their distribution, so that increasing plots from Abella-size to full-size tended to result in the inclusion of areas with lower densities. For example, at Shinob Kibe, almost 80 % of the plants were present in the Abella-size plots, which accounted for only 22 % of the area.

3.1.2. *Plant size, size class distribution, and flowering proportion*

When all plants in the full-size plots at each population in 2019 were binned by size (plant diameter) into 5 cm increments, size class distributions were all strongly right-skewed, with mean > median > modal plant diameters in every population, i.e., a majority of the plants were in the smaller size classes (Fig. 2). The likely reason for this is that a large proportion of the plants present established from seed in the wet spring of 2017 (two years previous). Mean plant diameter based on ANOVA with log transformed data was greatest at Tonaquint and White Dome and smallest at Shinob Kibe and Beehive Dome (TQ = WD > SK = BD based on means separation from ANOVA; Table A3) Among-population differences in diameter were also reflected in size class distributions (Fig. 2). Median and modal values were similarly high for Tonaquint and White Dome and lowest for Shinob Kibe.

Almost all the plants ≥6 cm in each population were in flower at the time of evaluation in May 2019 (94.0–96.9 %; Fig. 3). The great majority of non-flowering plants were concentrated in the two smallest size classes at each population, but many of the plants in even the smallest size class flowered. Only four plants out of a total of 1437 plants >20 cm in diameter across all populations were in non-reproductive status.

3.1.3. *Reproductive output and seed rain*

Plant diameter was significantly predictive of flower number at each of the four populations (Table 4). The best-fitting equations were second-order polynomial equations similar in general shape, showing exponential increase in maximum flower number as a function of maximum diameter (Fig. 4). Plant diameter explained from 67 to 91 % of the variation in flower number. These equations permitted estimates of flower number from flowering plant diameters measured in the imagery.

ANOVA results indicated that fruit set was high across all populations but differed significantly among populations (Table 5, Table A4a). There was also a highly significant difference among populations for mean number of seeds per capsule (Table A4b) with Beehive

Table 4
Polynomial regression equations relating plant diameter to maximum flower number at four *Arctomecon humilis* demography sites. Equations are of the form: maximum flower number = a + (b* plant diameter) + (c*(plant diameter + d)^2). (All regressions significant at P < 0.0001; see Fig. 4 for graphical representation).

	Beehive Dome	Shinob Kibe	Tonaquint	White Dome
Coefficient				
a	−149.267	−54.878	−117.984	−75.916
b	9.1131	6.1504	8.4398	6.3757
c	0.2468	0.0895	0.18414	0.11321
d	−27.227	−22.008	−26.936	−23.864
Sample size	99	98	106	98
R^2	0.867	0.909	0.886	0.674

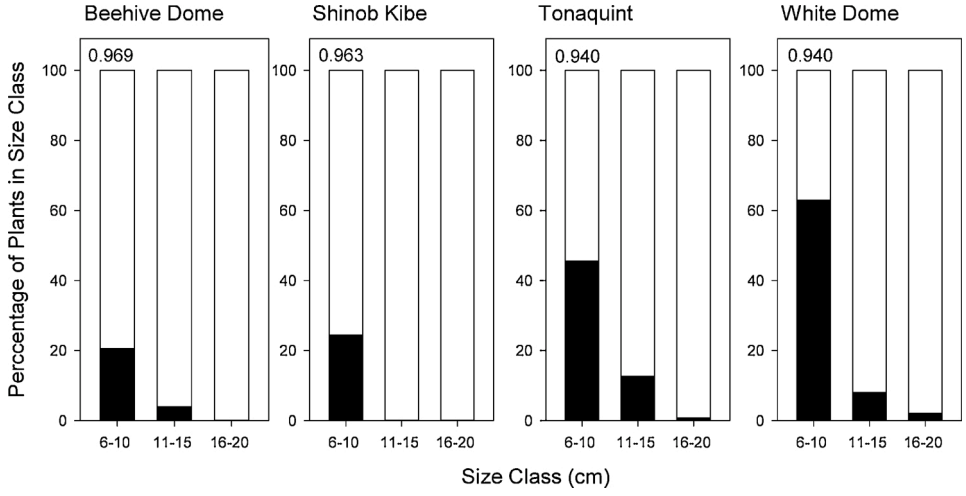

Fig. 3. Distribution of flowering and non-flowering plants in the three smallest size classes on full-size plots at four *Arctomecon humilis* populations in 2019. Numbers in the upper left-hand corner of each panel indicate proportion of total plants flowering at each population. (Black fill = non-flowering, white fill = flowering).

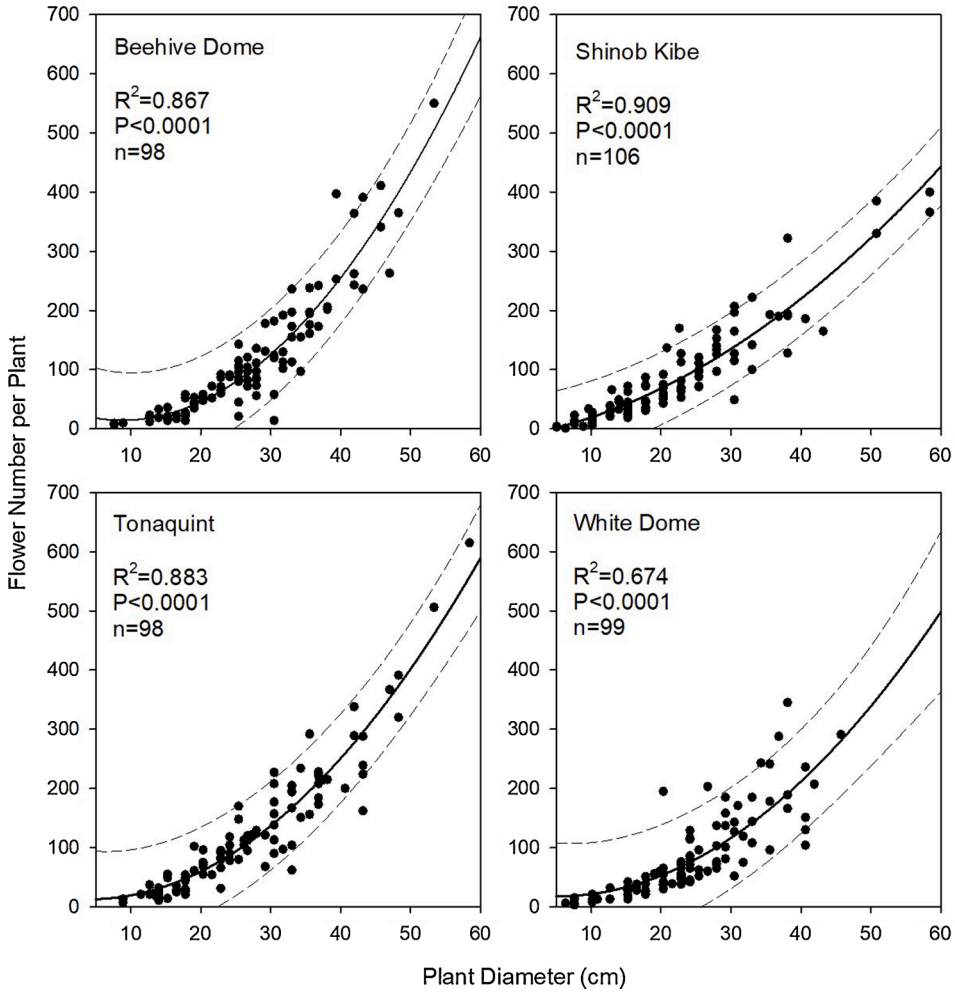

Fig. 4. Relationship between plant diameter and maximum flower number at each of four *Arctomecon humilis* populations fitted with polynomial equations shown in Table 5. Dashed lines represent the 95 % prediction interval from the analysis for each population.

Table 5
Means ± standard errors for fruits per flower (fruit set), seeds per fruit, and seeds per flower (the product of fruits per flower and seeds per fruit) at each of the four *Arctomecon humilis* demography sites in 2019. Seeds per fruit varied significantly among populations as indicated by means separations from ANOVA; fruit set (fruits per flower) varied little among populations but the population effect was nonetheless significant. Error bars represent standard error of the mean. (See Tables A4a and A4b for full analysis).

Population	Sample size	Fruits per flower	Seeds per fruit	Seeds per flower
Beehive Dome	94	0.994 ± 0.003a	23.8 ± 0.80a	23.6 ± 0.80
Shinob Kibe	99	0.980 ± 0.003b	14.6 ± 0.48b	14.3 ± 0.47
Tonaquint	94	0.976 ± 0.007bc	16.9 ± 0.84b	16.6 ± 0.84
White Dome	91	0.969 ± 0.005c	11.1 ± 0.90c	10.8 ± 0.87

Dome plants producing over twice as many seeds per capsule as White Dome plants. Plants at Tonaquint and Shinob Kibe produced similar intermediate numbers of seeds per capsule. The number of seeds per flower (fruits/flower *seeds/fruit) showed an identical trend because of the low variation in fruit set.

Estimated total seed production on the full-size plots was highest at Tonaquint at over 1.5 million seeds (Table 6; Table A5a; see ES2 for full data set). The total at Beehive Dome was second-highest at almost 1.2 million seeds, not significantly different from that at Tonaquint. Production at White Dome (ca. 650,000 seeds) was not significantly different from that at Shinob Kibe (ca. 320,000 seeds), but both were significantly lower than production at Beehive Dome or Tonaquint.

There was a strong effect of *a priori* density class on seed production, with the high-density plots producing more than four times the number of seeds produced on low-density plots across all populations (Table 6, Table A5a). The population by density class interaction was only marginally significant, and the directional trend for lower seed production at lower density was the same in each population.

Mean seed production per plant followed the same population rank order as mean seed number per capsule (Beehive Dome>>Tonaquint > Shinob Kibe>>White Dome; Table 5, Table A5b), showing that this factor was of overriding importance in seed production at the plant level. Beehive Dome had over twice the seed production per plant compared to White Dome.

The low total production at Shinob Kibe was largely a result of somewhat smaller area combined with the much lower plant density that resulted from including unoccupied habitat within the plots, as its mean seed production per plant was only slightly lower than Tonaquint and Beehive Dome. In contrast, the lower total production at White Dome was largely due to the lower production per plant, as densities were similar to those at populations with much higher total seed production.

The relationship between plant diameter and flower number per plant resulted in exponentially higher seed production as a function of plant size. When proportion of total seed production is plotted as a

Table 6
Estimated total seed production summed across nine monitoring plots for each population, summed across three replicates for each of three density classes within each population, and summed for each density class across all populations, estimated seed rain per square meter, and mean number of seeds per flowering plant for each population. *A posteriori* means separation tests for significant differences ($P < 0.05$) in total seed production among populations and among density classes are based on two-way ANOVA with seed production per plot as the replicate. The means separation test for the significance of differences among populations ($P < 0.05$) for mean seed number per flowering plant are from one-way ANOVA with individual plant as the replicate (See Tables A5a and A5b for full analysis).

Population	Total area (ha)	Total no. flowering plants	Estimated total seed production	Estimated total seed production per *a priori* density class			Estimated seed rain-m^{-2}	Mean seed number per flowering plant
				Low	Med	High		
Beehive Dome	5.40	727	1,174,689a	248,344	401,881	524,464	21.8	1616a
Shinob Kibe	4.13	260	322,623b	25,299	92,871	204,453	7.8	1241c
Tonaquint	5.40	1,029	1,546,578a	148,943	573,980	823,649	28.6	1503b
White Dome	5.40	870	656,586b	42,397	128,044	486,145	12.2	755d
Total	20.33	2,886	3,700,476	464,983c	1,196,776b	2,038,711a		

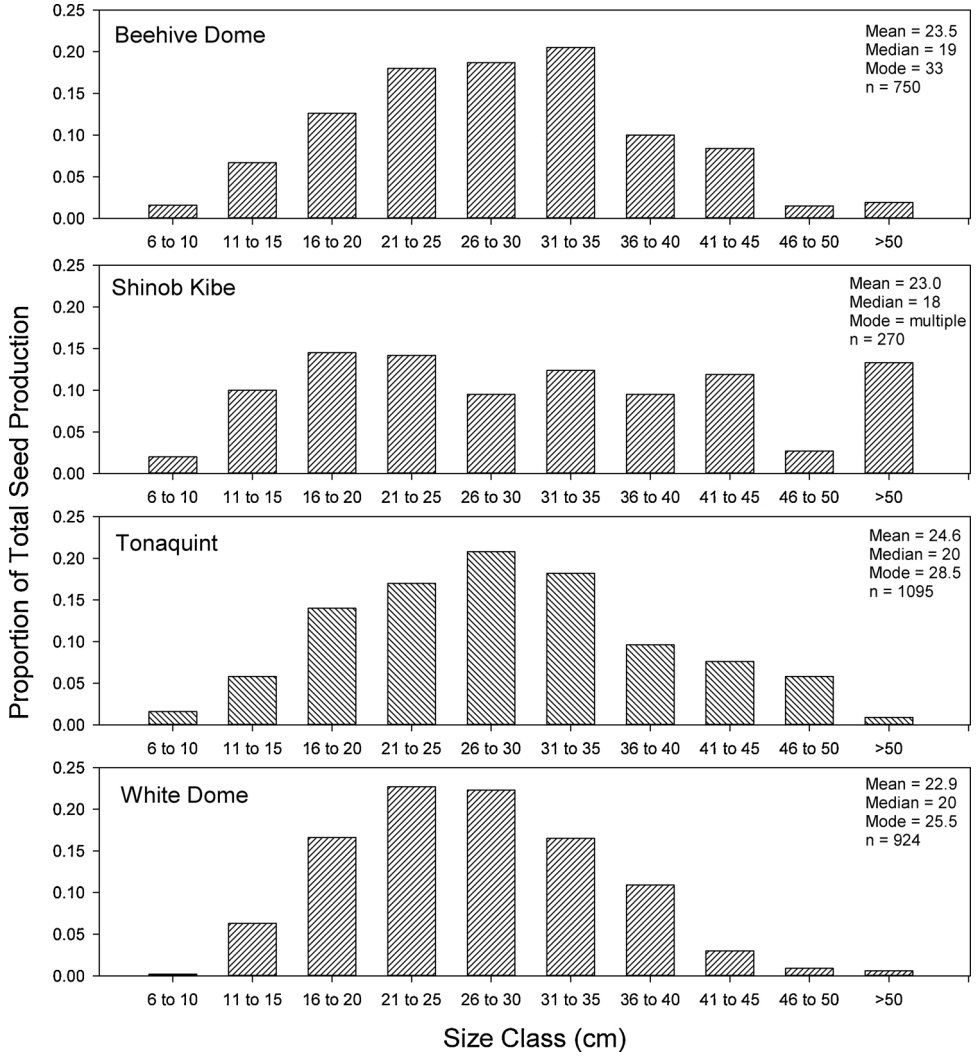

Fig. 5. Proportion of the estimated total 2019 seed production on full-size demography plots produced by all plants in each of ten size classes at four populations of *Arctomecon humilis*. Size classes that exhibited mean, median, and modal seed production values are presented on the graph for each population.

function of size class at each population, the resulting histograms look very different from the size class histograms. Instead of a strong right skew (Fig. 2), three of the four populations (Beehive Dome, Tonaquint, and White Dome) have seed production histograms that more closely resemble normal distributions (Fig. 5). This is because larger plants compensated for their lower numbers by producing exponentially more seeds per plant. The modal value for seed production shifted to a larger size class relative to the modal value for plant diameter in all three cases. The median size class was the same for plant diameter and seed production because seed production was calculated directly from plant

Table 7
Demographic information collected across two years (2018 and 2019) for Abella plots (0.1 ha) at White Dome and for full-size plots at Shinob Kibe. Error bars represent standard error of the mean.

Demographic measure	White Dome 0.1 ha plots	Shinob Kibe Full-size plots
Total recruited plant number in 2018	665	218
Survival from 2018–2019	392 (58.9 %)	194 (89.0 %)
New recruitment 2018–2019 [a]	61	76
Total recruited plant number in 2019	453	270
% plants flowering 2018	72.8 %	NA
% plants flowering 2019	97.1 %	96.3 %
Mean diameter (cm) in 2018	16.12 ± 0.33	12.06 ± 0.51
Mean 2018 diameter (cm) of plants that survived to 2019	14.97 ± 0.39	12.13 ± 0.56
Mean 2018 diameter (cm) of plants that did not survive	17.77 ± 0.55	11.48 ± 0.96
Mean 2019 diameter (cm) (including new recruits)	20.74 ± 0.37	20.66 ± 0.69
Mean proportional growth (2019 diameter/2018 diameter)	1.875	2.270
Mean growth interval (2019 diameter - 2018 diameter)	7.12 ± 0.37	10.51 ± 0.44
Percentage that regressed in size from 2018–2019	14.3 %	2.2 %

[a] New recruits are plants that were too small to score definitively as poppies (<6 cm) in 2018 but present as recruits in the 2019 imagery.

diameter. Because a large proportion of the plants were small, the median size class for seed production was also relatively small. Similarly, the mean size class for seed production was small, because the mean seed production was low due to the large number of small plants included in the calculation. This resulted in mode > mean > median for three populations (Fig. 2). The case of Shinob Kibe is unique in that there is no clear modal size class value for seed production as a function of size class, possibly because of smaller sample size (Fig. 5).

Seed production expressed on an area basis is an estimate of seed rain, a population-level demographic measure that is useful in predictions of population change over time. Average seed rain-m^{-2} in these four populations varied over a 3.7-fold range (Table 6). Comparing these seed rain densities to plant densities on an area basis puts them into perspective. At the average density across all full-size plots at all sites (144 plants ha^{-1}; Table 2), plant density was 0.0144 plants m^{-2} or 1.44 plants per 100 m^2. Even at these very low average plant densities, the average seed rain per 100 m^2 on the monitoring plots was estimated at 1,760 seeds.

3.2. Two-year study (2018–2019)

Following individual plants across years revealed similarities but also strong demographic contrasts between the two populations. At Shinob Kibe, survival of recruited plants from spring 2018 to spring 2019 was 89 %, while at White Dome survival was only 59 % (Table 7). Recruitment into the smallest detectable size class (6−10 cm) from 2018–2019 was evident at both populations, making up 13.5 % of the plants present at White Dome and 27.9 % of the plants present at Shinob Kibe in 2019. Flowering at White Dome in 2018 averaged only 73 % while most adult plants flowered at Shinob Kibe that year (DeNittis, 2018). In 2019 the proportion of plants that flowered was high in both populations (>96 %).

Mean plant diameter in 2018 was larger at White Dome than at Shinob Kibe, whereas in 2019 plants in the two populations were similar in mean diameter (Table 7). Size class distribution in 2018 was more strongly right-skewed at Shinob Kibe than at White Dome (Fig. 6). This trend was still somewhat evident in 2019 although the modal size class

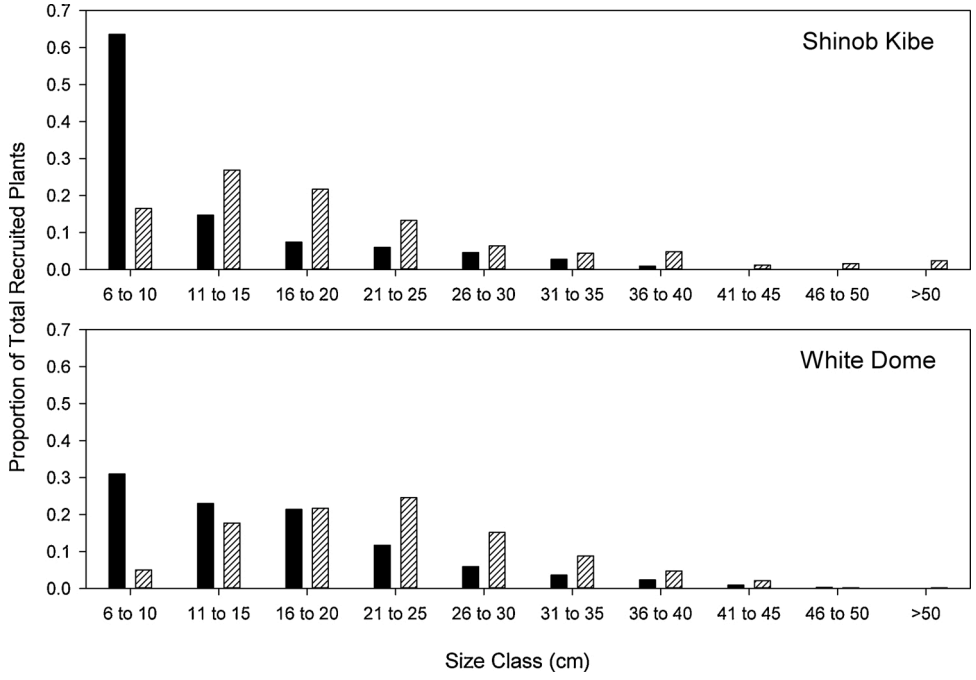

Fig. 6. Size class distributions in 2018 and 2019 for full-size plots at Shinob Kibe and for Abella (0.1 ha) plots at White Dome. (Black bars = 2018, white bars = 2019).

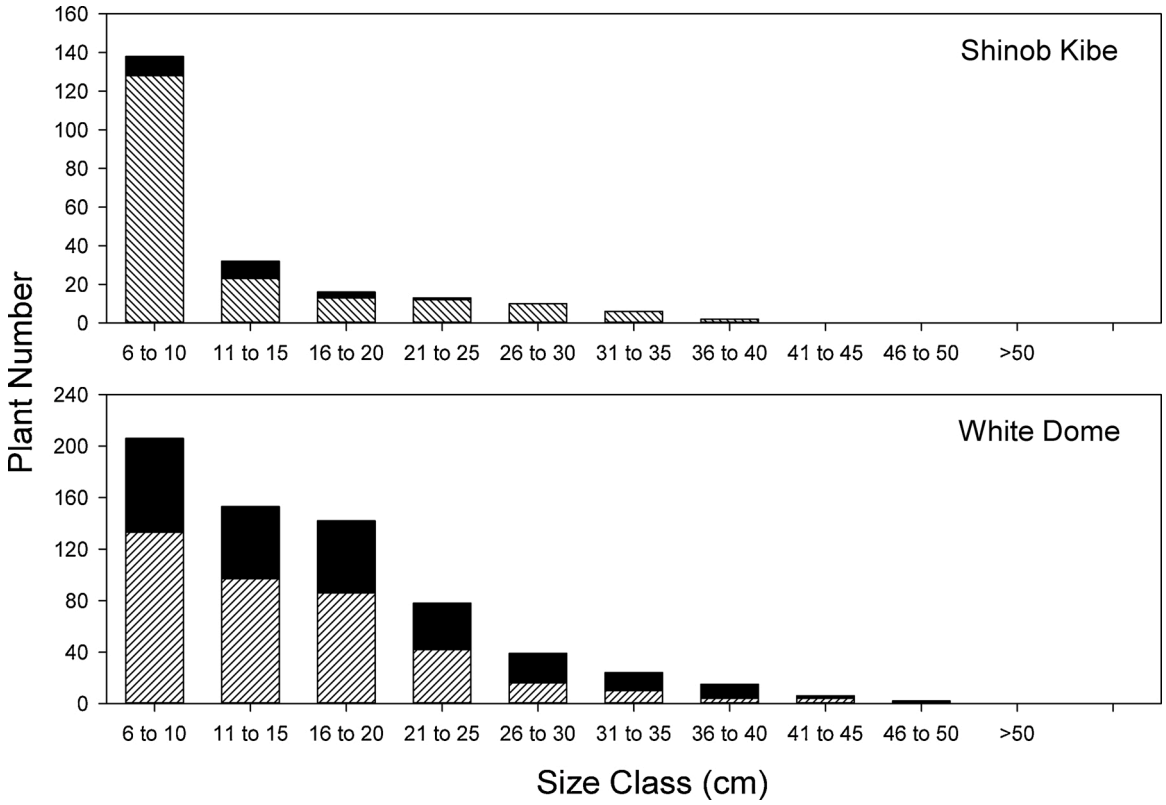

Fig. 7. Survival vs. mortality from 2018 to 2019 by size class in 2018 for the Shinob Kibe full-size plots and the White Dome Abella (0.1 ha) plots. (Black fill = non-surviving plants, hatched fill = surviving plants).

in both populations increased relative to 2018, reflecting overall plant size increase as plants from the 2017 establishment event grew to maturity. The few plants that did not survive at Shinob Kibe tended to be concentrated in the smaller size classes, while at White Dome larger plants were at higher risk of mortality (Fig. 7). Plant diameter in 2018 for plants that died at White Dome averaged almost 3 cm larger than diameter for plants that survived, a trend not seen at Shinob Kibe (Table 7). Surviving plants at White Dome also grew less than those at Shinob Kibe (7 cm vs 10.5 cm mean diameter increase) and more of the surviving plants regressed to a smaller size. Growth was inversely proportional to 2018 diameter in both populations, with the smallest plants sometime increasing in diameter as much as 5- to 6-fold (Fig. 8). The trend for slower growth in the larger size classes was more evident at White Dome than at Shinob Kibe, with many of the larger plants remaining static or regressing.

4. Discussion

This study has demonstrated the utility of drone-based imagery for generating demographic data for an endangered desert perennial plant. It was possible to locate and evaluate many hundreds of individuals scattered over several hectares at each population with minimal ground disturbance, an important advantage in the fragile habitat where dwarf bear poppy occurs. A demographic study at this scale would be difficult to achieve using conventional on-the-ground methodology even if surface disturbance were not an issue. Our methodology for demographic studies with drone imagery is still in the early stages of development, but this investigation has shown that such studies are feasible.

We recognize that our current image interpretation methodology has limitations. Characterizing plant size using maximum diameter is inherently imprecise because poppy plants are not consistently round but vary in shape. This is especially true for larger plants, which often show partial mortality and irregular outlines. This irregularity adds error to diameter measurements both in the imagery and in the field. The problem can be particularly severe in determining the relationship of maximum diameter to flower number. The fit of the polynomial regression equations was heavily influenced by values for larger plants, which showed high variance and were also generally under-represented in the sample, especially at White Dome where few plants survived to large size. Attempting more complex measurements did little to rectify the problem, but we have found in later studies that stratified sampling by plant size results in polynomial equations with better fit that are also very similar across populations and years. We also want to emphasize that our seed production numbers are estimates, not measurements, as there are many potential sources of error involved in these calculations. These estimates apply only to the monitoring plots in each population and cannot be extrapolated to the population level without a more considered treatment of plant density effects across the entire population.

We were able to detect and quantify differences among populations for many demographic parameters, including density, size class distribution, and flowering proportion, with only a single year of drone imagery. By including small-scale reproductive output sampling on the ground at each population, we were also able to estimate seed production per plant and seed rain over several hectares. This window into the seed bank is especially important for dwarf bear poppy, a relatively short-lived species that relies on a long-lived seed bank and episodic seedling recruitment in exceptionally favorable years for population persistence (Harper & Van Buren, 2004; Meyer et al., 2015).

By examining imagery obtained across two years, we demonstrated

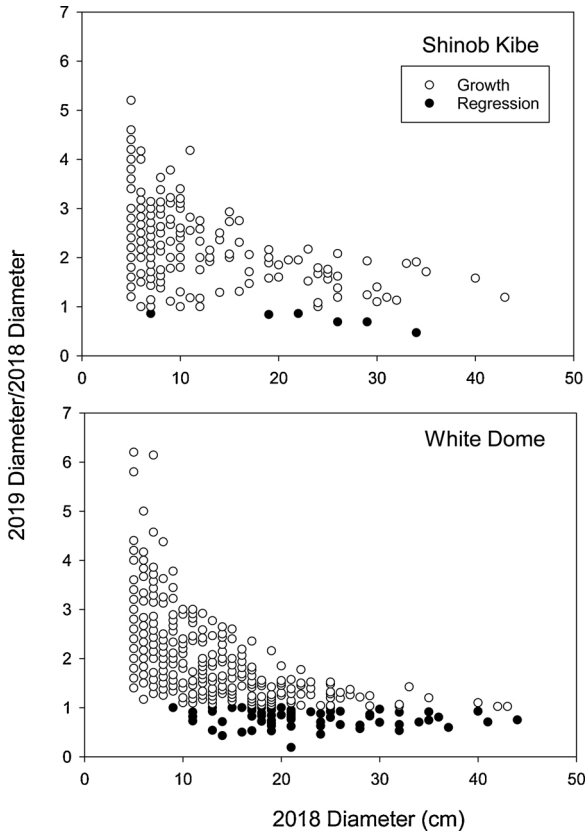

Fig. 8. Proportional growth (2019 diameter/2018 diameter) for surviving plants in 2019 plotted as a function of diameter in 2018 for full-size plots at Shinob Kibe and for Abella (0.1 ha) plots at White Dome. Plants recruited in 2019 were included as 5.0 cm in diameter in 2018.

that valuable information on recruitment, survival and growth as a function of size class could easily be obtained, and that between-population demographic differences were readily detected. Determining whether these population contrasts reflect differential responses to current-year conditions or differences in long-term trends will require additional years of study. We initiated our drone-based census and demographic study project after the major dwarf bear-poppy seedling establishment event in 2017, in order to follow the fate of this cohort across multiple years. Post-establishment patterns of survival, growth, and reproductive output are already becoming evident. We will continue evaluation of full-size plots at these four populations for at least two more years, effectively extending our one-year study into a multiple-year demographic analysis on a relatively large scale. The information we gain will be used to improve our current population viability analysis for this species, which was based on demographic data from a single small sample area (0.07 ha; Harper & Van Buren, 2004; Meyer et al., 2015).

We also intend to streamline the process of image acquisition, processing, and interpretation to the point that the methodology will potentially be usable by non-researchers. This will include developing a deep learning approach for poppy detection and evaluation in the imagery, eliminating one of the most time-intensive and subjective steps. We will also optimize the collection of reproductive output data, once we learn how much these relationships vary by year. The goal is to develop a simple, efficient procedure that managers or their contractors can carry out and that can be used to amass the extensive long-term data sets needed to understand population dynamics and management needs of dwarf bear poppy, as well as other endangered plant species.

Potential drawbacks to the drone-based approach include the legal and licensing requirements surrounding the use of drone technology, the need to master the software and hardware to become proficient at piloting drones in complex terrain, the necessity for processing and management of extremely large imagery databases, and the upfront cost of the necessary equipment to capture, process, and analyze imagery. However, even with visual assessment as described here rather than use of deep learning methods to find and evaluate plants in the imagery, the total time investment is probably less than the time required to collect and process equivalent datasets obtained on the ground. Field time is definitely substantially reduced using the drone-based approach (Abella, 2012, 2014). Another advantage is that, once the imagery is acquired, the remaining steps are not dependent on completion while the field populations are in the appropriate phenological stage.

The drone-based methodology we have described can be applied to many other plant species of conservation concern, especially those that occur in sparsely vegetated habitats. As mentioned earlier, large numbers of rare plant species are edaphic endemics that occur in 'badlands' settings where both plant density and diversity tend to be low. This suggests that drone-based monitoring may be a good approach to reducing field-related monitoring costs and labor for many of these species, while acquiring robust demographic data sets over large areas that would be extremely difficult to obtain using traditional methods.

Declaration of Competing Interest

The authors declare that they have no known competing financial interests or personal relationships that could have appeared to influence the work reported in this paper.

Acknowledgments

This project was carried out with the aid of funding to Utah Valley University through Grant # F104790 from The Nature Conservancy and through Challenge Cost Share Grant # F19AP00568 from the US Fish and Wildlife Service. We thank Jena Lewinsohn of USFWS and Elaine York of TNC for their unflagging support of our work. Special thanks to Michael Stevens of Utah Valley University for handling funding logistics. Sydney Houghton and Eli Hartung of Utah Valley University helped with reproductive output sample processing and drone image interpretation, and Suzette Clement of the US Forest Service Shrub Sciences Laboratory performed seed viability analysis.

Appendix A. Statistical analyses in support of the results presented in the main manuscript

Table A1
Two-way ANOVA testing the significance of population (SITE) and *a priori* density class (DCLASS) main effects and their interaction on *A. humilis* density. Density data were log-transformed to improve normality and homogeneity of variance prior to analysis. Analysis was performed in SAS Version 9.4 Proc GLM.

Source	DF	Sum of Squares	Mean Square	F Value	Pr > F
Model	11	33.73545671	3.06685970	8.45	<.0001
Error	24	8.70973071	0.36290545		
Corrected Total	35	42.44518742			
Source	**DF**	**Type I SS**	**Mean Square**	**F Value**	**Pr > F**
SITE	3	9.50059596	3.16686532	8.73	0.0004
DCLASS	2	21.54428700	10.77214350	29.68	<.0001
SITE*DCLASS	6	2.69057375	0.44842896	1.24	0.3233

Table A2
Three-way ANOVA testing the significance of population (SITE), plot size (AREASIZE) and density class (DCLASS) and their interactions on *A. humilis* density at two sites (White Dome and Shinob Kibe). Density data were log-transformed to improve normality and homogeneity of variance prior to analysis. Analysis was performed in SAS Version 9.4 Proc GLM.

Source	DF	Sum of Squares	Mean Square	F Value	Pr > F
Model	11	60.59628232	5.50875294	5.95	0.0001
Error	24	22.21742662	0.92572611		
Corrected Total	35	82.81370894			

Source	DF	Type III SS	Mean Square	F Value	Pr > F
SITE	1	2.48316937	2.48316937	2.68	0.1145
DCLASS	2	47.66394256	23.83197128	25.74	<.0001
SITE*DCLASS	2	0.51976458	0.25988229	0.28	0.7577
AREATYPE	1	7.47328065	7.47328065	8.07	0.0090
SITE*AREATYPE	1	0.62670467	0.62670467	0.68	0.4187
DCLASS*AREATYPE	2	1.13070589	0.56535294	0.61	0.5512
SITE*DCLASS*AREATYPE	2	0.69871459	0.34935730	0.38	0.6896

Table A3
One way ANOVA testing the population main effect on mean diameter per plant.

Source	DF	Sum of Squares	Mean Square	F Value	Pr > F
Model	3	3.7518904	1.2506301	7.09	<.0001
Error	3035	535.3724008	0.1763995		
Corrected Total	3038	539.1242912			

Source	DF	Type I SS	Mean Square	F Value	Pr > F
POP	3	3.75189044	1.25063015	7.09	<.0001

Table A4a
One-way ANOVA to test the population main effect on fruit set (fruits/flowers) at four populations of *A. humilis*. Analysis was performed on binomial data in SAS 9.4 Proc Glimmix.

Type III Tests of Fixed Effects				
Effect	Num DF	Den DF	F Value	Pr > F
pop	3	396	15.68	<.0001

Table A4b
One-way ANOVA to test the population main effect on mean number of seeds per capsule at four populations of *A. humilis*. Analysis was performed in SAS 9.4 Proc GLM.

Source	DF	Sum of Squares	Mean Square	F Value	Pr > F
Model	3	7864.50520	2621.50173	47.72	<.0001
Error	374	20547.20772	54.93906		
Corrected Total	377	28411.71292			

Table A5a
Two-way ANOVA for the effects of population, density class, and their interaction on seed production per plot at four populations of *A. humilis* in 2019.

Source	DF	Sum of Squares	Mean Square	F Value	Pr > F
Model	11	230919523883	20992683989	10.15	<.0001
Error	24	49635587318	2068149471.6		
Corrected Total	35	280555111201			

Source	DF	Type III SS	Mean Square	F Value	Pr > F
POP	3	98178703302	32726234434	15.82	<.0001
DENSCLASS	2	103361775125	51680887563	24.99	<.0001
POP*DENSCLASS	6	29379045456	4896507576	2.37	0.0613

Table A5b
One-way ANOVA for the effect of population on mean seed production per plant at four populations of *A. humilis* in 2019.

Source	DF	Sum of Squares	Mean Square	F Value	Pr > F
Model	3	373613586	124537862	92.08	<.0001
Error	2882	3897903948	1352500		
Corrected Total	2885	4271517534			

Appendix B. Verification of the accuracy of plant maximum diameters measured in the drone imagery

To verify that plant maximum diameter measurements in the drone imagery were an accurate indication of plant maximum diameter in the field, we first obtained accurate GPS coordinates for all field-tagged plants from the 2019 reproductive study that we were able to locate at the Beehive Dome study site in April 2021 (n = 78). Remaining tags could not be located due to extensive rodent disturbance. We then matched these tags with known GPS locations for plants in the imagery. We regressed maximum diameter measured in the drone imagery on maximum diameter as measured in the field during flowering in 2019.

The resulting regression line (imagery diameter = 0.926*field diameter-0.554) had an adjusted R^2 value of 0.912 ($P < 0.0001$), an intercept near zero, and a slope near one, supporting the hypothesis of correspondence between the two sets of measurements (Fig. B1). The 95

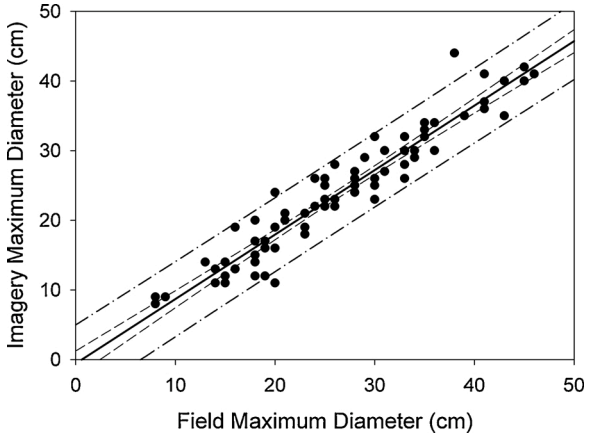

Fig. B1. The relationship between field-measured maximum plant diameter and imagery-measured maximum plant diameter for 78 flowering plants measured at the same time at Beehive Dome in 2019. The black line represents the regression line, the dashed bounding lines represent the 95 % confidence interval, and thedot-dash bounding lines represent the 95 % prediction interval.

% confidence interval is shown as dashed lines. It indicates that the regression line would fall within the bounds of this interval 95 % of the time. The 95 % prediction interval is shown as dot-dash lines. It indicates that for any randomly selected plant of a given field-measured maximum diameter, its corresponding imagery-measured maximum diameter would fall within the bounds of the prediction interval 95 % of the time.

As further confirmation of the equivalence of these two sets of measurements, we performed one-way ANOVA comparing mean diameter of field-measured plants (26.3 cm) and imagery-measured plants (23.9 cm). The means were not significantly different at $P < 0.05$ (d. f. = 1, 154, $F = 3.02$, $P = 0.0843$).

Appendix C. Supplementary data

Supplementary material related to this article can be found, in the online version, at doi:https://doi.org/10.1016/j.jnc.2021.126020.

References

Abella, S. (2012). *Monitoring dwarf bear poppy and siler pincushion Cactus at the white dome nature preserve* (p. 23 p.). Salt Lake City, UT: Salt Lake City Office. Report on file, The Nature Conservancy.

Abella, S. (2014). *2014 field monitoring and reporting for dwarf bearpoppy (Arctomecon humilis) and Siler pincushion Cactus (Pediocactus sileri) at the White Dome Nature Preserve, a nature conservancy property in Washington County* (p. 20 p.). Utah. Salt Lake City, UT: Salt Lake City Office. Report on file, The Nature Conservancy.

Anacker, B. L. (2014). The nature of serpentine endemism. *American Journal of Botany, 101*, 219–224.

Baena, S., Boyd, D. S., & Moat, J. (2018). UAVs in pursuit of plant conservation - real world experiences. *Ecological Informatics, 47*, 2–9.

Baena, S., Moat, J., Whaley, O., & Boyd, D. S. (2017). Identifying species from the air: UAVs and the very high resolution challenge for plant conservation. *PloS One, 12*. e0188714.

Buters, T. M., Belton, D., & Cross, A. T. (2019). Multi-sensor UAV tracking of individual seedlings and seedling communities at millimetre accuracy. *Drones, 3*, 81.

Cerrejón, C., Valeria, O., Marchand, P., Caners, R. T., & Fenton, N. J. (2021). No place to hide: Rare plant detection through remote sensing. *Diversity & Distributions*. https://doi.org/10.1111/ddi.13244.

Christie, K. S., Gilbert, S. L., Brown, C. L., Hatfield, M., & Hanson, L. (2016). Unmanned aircraft systems in wildlife research: Current and future applications of a transformative technology. *Frontiers in Ecology and the Environment, 14*, 241–251.

Cunliffe, A. M., Brazier, R. E., & Anderson, K. (2016). Ultra-fine grain landscape-scale quantification of dryland vegetation structure with drone-acquired structure-from-motion photogrammetry. *Remote Sensing of Environment, 183*, 129–143.

Dash, J. P., Watt, M. S., Paul, T. S. H., Morgenroth, J., & Hartley, R. (2019). Taking a closer look at invasive alien plant research: A review of the current state, opportunities, and future directions for UAVs. *Methods in Ecology and Evolution, 10*, 2020–2033.

DeNittis, A. M. (2018). *Hand pollination of the dwarf bear-poppy Arctomecon humilis population at Shinob Kibe* (p. 13 p.). Salt Lake City, UT: Salt Lake City Office. Report on file, The Nature Conservancy.

Elzinga, C. L., Salzer, D. W., Willoughby, J. W., & Gibbs, J. P. (2009). *Monitoring plant and animal populations: A handbook for field biologists* (p. 372 p.). Malden, Mass: John Wiley and Sons Ltd.

Escudero, A., Palacio, S., Maestre, F. T., & Luzuriaga, A. L. (2015). Plant life on gypsum: A review of its multiple facets. *Biological Reviews, 90*, 1–18.

Feduck, C., McDermid, G. J., & Castilla, G. (2018). Detection of coniferous seedlings in UAV imagery. *Forests, 9*, 432.

Fust, P., & Loos, J. (2020). Development perspectives for the application of autonomous, unmanned aerial systems (UASs) in wildlife conservation. *Biological Conservation, 241*, 108380.

Harper, K. T., & Van Buren, R. (2004). Dynamics of a dwarf bear-poppy (*Arctomecon humilis*) population over a sixteen-year period. *Western North American Naturalist, 64*, 482–491.

Harper, K. T., Van Buren, R., & Aanderud, Z. T. (2001). The influence of interplant distance and number of flowers on seed set in dwarf bear-poppy (*Arctomecon humilis*). In *Southwestern Rare and Endangered Plants: Proceedings of the Third Conference: September 25-28, 2000, Flagstaff, Arizona. Rocky Mountain Research Station Proceedings RMRS-P-23* (pp. 105–109).

Leduc, M. B., & Knudby, A. (2018). Mapping wild leek through the forest canopy using a UAV. *Remote Sensing, 10*, 70.

Menges, E. S., & Gordon, D. (1996). Three levels of monitoring intensity for rare plant species. *Natural Areas Journal, 16*, 227–237.

Meyer, S. E., Van Buren, R., & Searle, A. (2015). Plant demography study and population viability analysis for the endangered dwarf bear poppy (*Arctomecon humilis*). *Report on file, the nature conservancy*. Salt Lake City, UT: Salt Lake City Office.

Ooi, M., Auld, T., & Whelan, R. (2004). Comparison of the cut and tetrazolium tests for assessing seed viability: A study using Australian native *Leucopogon* species. *Ecological Management and Restoration, 5*, 141–143.

Ouyang, J., Simonson, S. L., Zhang, Y., Zhuang, C., Wang, J., Chen, Z., et al. (2020). Using UAV technology for basic data collection of *Firmiana danxiaensis* H. H. Hsue & H. S. Kiu, J. S. (Malvaceae), an important, nationally protected wild plant in Zhanglao Peak, Danxiashan Mountain, South China. In *IOP Conference Series: Earth and Environmental Science, 467* p. 012130).

Palmer, M. E. (1987). A critical look at rare plant monitoring in the United States. *Biological Conservation, 39*, 113–127.

Pérez-García, F. J., Martínez-Hernández, F., Mendoza-Fernández, A. J., Merlo, M. E., Sola, F., Salmerón-Sánchez, E., et al. (2017). Towards a global checklist of the of world gypsophytes: A qualitative approach. *Plant Sociology, 54*, 61–76.

Portman, Z. M., Tepedino, V. J., Tripodi, A. D., Szalanski, A. L., & Durham, S. L. (2018). Local extinction of a rare plant pollinator in Southern Utah (USA) associated with invasion by Africanized honey bees. *Biological Invasions, 20*, 593–606.

Rominger, K. (2018). *Population survey and monitoring for the dwarf bear-poppy (Arctomecon humilis) on the White Dome and Shinob kibe preserves*. Salt Lake City, UT: Salt Lake City Office. Report on file, The Nature Conservancy.

Rominger, K. (2019a). *Dwarf bear-poppy census and habitat evaluation at Beehive Dome*. Salt Lake City, UT: Bureau of Land Management Utah State Office. Report on file.

Rominger, K. (2019b). *Dwarf bear-poppy (Arctomecon humilis) detection protocol and census in the tonaquint block area of the red bluffs population*. Salt Lake City, UT: Utah Department of Natural Resources. Report on file.

Rominger, K., & Meyer, S. (2019). Application of UAV-based methodology for census of an endangered plant species in a fragile habitat. *Remote Sensing, 11*, 719.

Sanchez-Bou, C., & Lopez-Pujol, J. (2014). The coming revolution: The use of drones in plant conservation. *Collectanea Botanica, 33*(e007), 1–4.

Strumia, S., Buonanno, M., Aronne, G., Santo, A., & Santangelo, A. (2020). Monitoring of plant species and communities on coastal cliffs: Is the use of unmanned aerial vehicles suitable? *Diversity, 12*, 149.

Tepedino, V. J., Mull, J., Griswold, T. L., & Bryant, G. (2014). Reproduction and pollination of the endangered dwarf bear-poppy *Arctomecon humilis* (Papaveraceae) across a quarter century: Unraveling of a pollination web? *Western North American Naturalist, 74*, 311–324.

United States Fish and Wildlife Service. (1979). Endangered and threatened wildlife and plants: Rule to determine *Arctomecon humilis* is an endangered species. *Federal Register, 44*, 64250–64252.

United States Fish and Wildlife Service. (2016). *Dwarf bear-poppy. Arctomecon humilis Coville. Five-year review: Summary and evaluation* (pp. 1–55). Salt Lake City, UT: US Fish and Wildlife Service, Utah Field Office.

Van Auken, O. W., & Taylor, D. L. (2017). Using a drone (UAV) to determine the *Acer grandidentatum* (bigtooth maple) density in a relic, isolated community. *Phytologia, 99*, 208–220.

Willis, C. K., Cowling, R. M., & Lombard, A. T. (1996). Patterns of endemism in the limestone flora of South African lowland fynbos. *Biodiversity and Conservation, 5*, 55–73.

Zweig, C. L., Burgess, M. A., Percival, H. F., & Kitchens, W. M. (2015). Use of unmanned aircraft systems to delineate fine-scale wetland vegetation communities. *Wetlands, 35*, 303–309.